Int J Energy Environ Eng (2014) 5:349–356
DOI 10.1007/s40095-014-0131-3

ORIGINAL RESEARCH

Carbon dioxide adsorption on zeolites and activated carbon by pressure swing adsorption in a fixed bed

Lalhmingsanga Hauchhum · Pinakeswar Mahanta

Received: 12 February 2014 / Accepted: 10 June 2014 / Published online: 2 August 2014

Abstract Combustion of fossil fuels is one of the major sources of greenhouse gas (GHG) CO_2, it is therefore necessary to develop technologies that will allow us to utilize the fossil fuels while reducing the emissions of GHG. Removal of CO_2 from flue gasses has become an effective way to mitigate the GHG and adsorption is considered to be one of the methods. Adsorption of CO_2 on zeolite 13X, zeolite 4A and activated carbon (AC) have been investigated at a temperature ranging from 25 to 60 °C and pressure up to 1 bar. The experimental data were fitted with isotherm models like Langmuir and Freunlich isotherm model. The Langmuir model fit well with the two zeolites and Freunlich model fit well with AC. The thermodynamics parameters were calculated and found to be exothermic in natures for all three adsorbents. Moreover, regeneration studies have been conducted in order to verify the possibility of activated carbon reutilization, to determine its CO_2 adsorption capacity within consecutive cycles of adsorption–desorption. Temperature swing adsorption was employed as the regeneration method through heating up to a temperature of approximately 100 °C. There is no full reversibility for zeolites while AC can achieve complete regenerations.

Keywords Adsorption · Carbon dioxide · Thermodynamic parameters · Activated carbon · Zeolite

L. Hauchhum (✉) · P. Mahanta
Department of Mechanical Engineering, Indian Institute of Technology Guwahati, Guwahati 781039, Assam, India
e-mail: h.sanga@iitg.ernet.in

P. Mahanta
e-mail: pinak@iitg.ernet.in

Introduction

The emission of gaseous products of combustion into the atmosphere, mainly Carbon dioxide (CO_2) is regarded as a major cause of global warming and climate change, through the so-called greenhouse effect [1]. Currently, 85 % of total world demanded energy is supplied by thermal power plants fed by fossil fuels, including coal, oil and gas. They account for about 40 % of total CO_2 emissions [2]; Yang et al. [3]; [4]. Among the ways to control, reduce or mitigate this effect, the capture of CO_2 from flue gasses of industrial combustion processes and its storage in deep geological formations is now being considered as a serious option [5–7].

A number of adsorption processes are used commercially for adsorbent process, including pressure swing adsorption (PSA), vacuum pressure swing adsorption (VPSA), and thermal or temperature swing adsorption (TSA). A number of research works have been done using the processes mentioned above on different types of adsorbent materials. Recent developments have demonstrated that PSA is a promising option for separating CO_2 due to its ease of applicability over a relatively wide range of temperature and pressure conditions, its low energy requirements, and its low capital investment cost (Agarwal et al. [8]). Many studies concerning CO_2 removal from various flue gas mixtures by means of PSA processes have been addressed in the literature. Prior to the design of an adsorption process, selecting an appropriate adsorbent with high selectivity and working capacity, as well as a strong desorption capability, is key to separating CO_2. As a result, a wide variety of adsorbents like activated carbon, zeolites, silica gel, activated alumina, urea–formaldehyde and melamine–formaldehyde resins, poly-ethyleneimine and hollow fiber carbon membranes based adsorbents, etc. have

been investigated for this purpose [9]; Sircar et al. [10]; [11, 12, 17]. Recent development shows an improvement in adsorbent materials with higher adsorption capacity and selectivity like Activated carbon honeycomb monolith—Zeolite 13X hybrid system, zeolites NaKA and nano-NaKA, FAU zeolites and zeolite 13X prepared from bentonite [13–16].

The PSA process is based on preferential adsorption of the desired gas on a porous adsorbent at high pressure, and recovery of the gas at low pressure. Thus, the porous sorbent can be reused for subsequent adsorption. PSA technology has gained interest because of the low energy requirements and low capital investment costs. The low recovery rate of CO_2 is one of the problems reported with the PSA process [18]. Development of regenerable sorbents that have high selectivity, adsorption capacity, and adsorption/desorption rates for CO_2 capture is critical for the success of the PSA process. Cost of the sorbent is also a major factor that needs to be considered for the process to be economical [19, 20].

The adsorption method of choice for many zeolite molecular sieves is PSA, although some experiments have employed a combined pressure and temperature swing adsorption (PTSA) process (Ruthven et al. [21]; [22, 23]. It has been reported that a particular TSA and PSA cycle conditions would result in higher expected working capacity with an increase in feed temperature. Zeolites have shown promising results for the separation of CO_2 from gas mixtures and can potentially be used for the PSA process. Natural zeolites are inexpensive and can be viable sorbents if they work for the process application [24]. It has also been reported that using AC as an adsorbent material, the adsorption capacity can increase till 30 Bar and become steady after 30–35 bars [25].

Based on the literatures available, PSA seems to be the best option for separating CO_2 from flue gas due to its ease of applicability over a relatively wide range of temperature and pressure conditions. A number of sorbents like zeolite, activated alumina, activated carbons, etc. have been utilized and cost of the sorbents play a vital role for the process to be economical. In this paper, low cost and abundantly available locally, coconut fiber based AC was employed as the sorbent materials and compared with commercial zeolites. Work had been done to develop a process in which CO_2 was adsorbed from a gas stream containing $\sim$13.8 vol. % of CO_2 onto zeolite 13X, zeolite 4A and AC by means of PSA process. The system was tested for five different adsorption and desorption cycles in order to determine the adsorbent bed's regeneration efficiencies. Kinetics and adsorption thermodynamics parameters have also been calculated.

Materials and methods

Materials

The properties of commercial zeolite 13X and Zeolite 4A which were purchased from the local chemist are given in Table 1. While the AC (coconut fiber) used was obtained from a local area. It was peeled and the fibrous part was collected and was broken into small pieces. The coconut fibre was washed with water, dried in the sun for 10 h and transferred to the furnace. The coconut pieces were burnt distinctively in the furnace for an hour at a temperature of 350 °C. The charcoal produced was withdrawn from the furnace and sieved; a mean particle diameter of 0.92 mm was obtained. The material characterization was done for proximate and ultimate analysis and details of the physical and chemical properties are given in Table 2.

Table 1 Properties of zeolites

Properties	4A	13X
BET surface area (m^2/g)	434	720
Pore diameter (Å)	4.0	10.0
Bulk density (kg/m^3)	700	639
Particles diameter (mm)	1.5	2
Composition (wt %)		
Sodium	10.8	11.9
Aluminum	13.6	14.3
Silicon	16.1	17.8
Calcium	0.8	0.6
Potassium	0.9	0.2
Magnesium	1.2	1.3

Table 2 Properties of activated carbon

BET surface area (m^2/g)	214
Pore volume (cc/g)	0.068
Bulk density (kg/m^3)	350
Particles diameter (mm)	0.92

Ultimate analysis (wt %)

C	O	Cl	K
41.28	36.00	6.01	33.71

Proximate analysis (wt %)

Ash	Moisture	Fixed carbon	Volatile
4.8	10.63	14.49	70.08

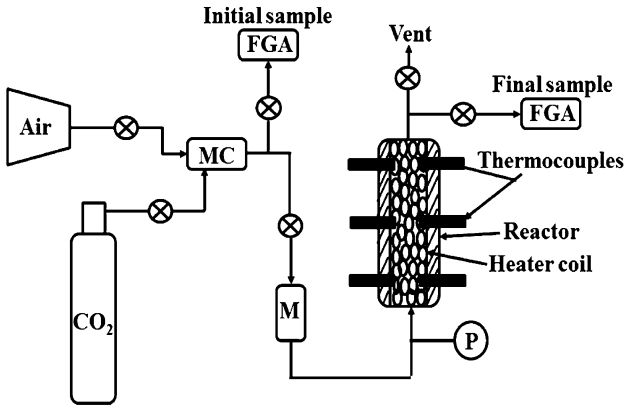

Fig. 1 Schematic of the experimental set-up for fixed bed. *MC* mixing chamber, *M* mass flow meter, *P* pressure gage, *FGA* flue gas analyzer

Table 3 Experimental conditions

Bed weight	20 g
Reactor length	200 mm
Reactor diameter	30 mm
Influent CO_2 concentration	13.8 vol. %
Inlet flow rate	15 LPM
Bed porosity	0.5
Superficial velocity	0.13 m/s
Adsorption temperature	25–60 °C
Adsorption total pressure	1 bar

Methods

The experimental set-up for the adsorption test consists of a CO_2 cylinder and Gas Compressor interconnected through a pipe to the system as shown in Fig. 1 based on [25]. The Gas Compressor could provide sufficient pressure up to 10 kg/cm^2 with a discharge capacity of 84 LPM. The gas mixing chamber was made up of a GI pipe of 20 mm diameter and 80 mm in length to achieve the required mixture of air and CO_2 (13.8 vol. %) at a constant rate. Ceramic wool was wrapped around the reactor above the heater coil for insulation. Thermocouples (K-type) were inserted in the bed to measure the bed temperatures with accuracy of ±0.5 %.

A Glass Tube Rotameter of the range 0–35 LPM was used to control the mass flow rate and measure the mass flow rate of the incoming gas. The reactor was made up of GI pipe with 30 mm diameter with 1.5 mm wall thickness and 200 mm in height. A pressure monitoring system was attached to know the incoming pressure and experiments were carried at varying pressure to see the effect of pressure in the adsorption process at a constant temperature. A number of needle valves were attached in the system to control the system operation at the require rate. Flue Gas Analyzer (KM9106) was used to measure the inlet sample gas and the outlet gas properties. The apparatus was tested for leak absence and for accuracy through calibrations with an empty tank. Table 3 give details of the operating parameters.

The process employed a single-bed PSA unit. For the adsorption process, first the air was allowed to flow through the reactor and then followed by carbon dioxide. To maintain equal flow rate and pressure of both the flows, the gas mixture was allowed to pass through the mixing chamber. The flow of air was then stopped and allowed only the pure CO_2 to flow through the reactor for measurement of the mass of CO_2 adsorbed per the mass of the adsorbent. To know the effective adsorbed mass on the adsorbent materials, $Q_{eff,}$ two quantities were defined: Q_t that is the mass containing the reactor including the adsorbents and Q_d which is the mass of the empty reactor or dead volume. The Q_{eff} was then calculated with the equation as follows: $Q_{eff} = Q_t - Q_d$.

Results and discussions

Adsorption breakthrough curves

Adsorption is a transient process and the amounts of material adsorbed within a bed depend both on position and time. The CO_2 breakthrough curves for the three adsorbents are shown through Figs. 2, 3, 4 and the experimental conditions are given in Table 3. The breakthrough curves show ratio of the outlet concentration and the influent concentration against the contact time at an atmospheric pressure, and at a temperatures of 25, 35, 45 and 60 °C. The general pattern of the breakthrough curves were achieved as expected for all adsorbents. For zeolite 13X, the adsorption breakthrough occurs at 20 min and for zeolite 4A, the adsorption breakthrough occurs at 16 min.

This shows that the pore diameter of zeolite 13X (10 Å) and zeolite 4A (4 Å) is sufficient for the CO_2 to enter into the zeolites channels. The major cations of zeolites are Na and K and this major cation appears to play a main role in the adsorption of CO_2. Also, sodium appears to be the favorable cation for the adsorption of CO_2. The saturation time for zeolite 13X is longer than that of zeolite 4A which is due to the larger pore volume. For AC, the breakthrough time is 8 min at 25 °C. The breakthrough time with AC was shorter as compared to zeolites, indicating that the CO_2 adsorption capacity of AC is lower than that of zeolites. The differences in adsorption observed with zeolites and AC should be related to the differences in the chemical nature at the surface and porosity. Both the zeolites have higher surface area than AC and that may have contributed to the higher adsorption capacity of zeolites.

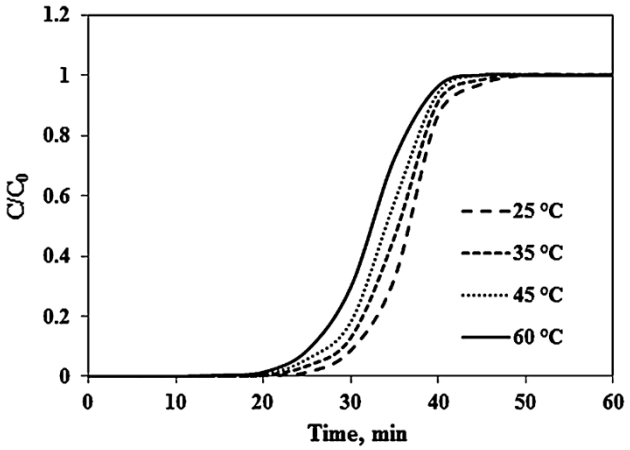

Fig. 2 CO_2 breakthrough curve for zeolite 13X at 1 bar

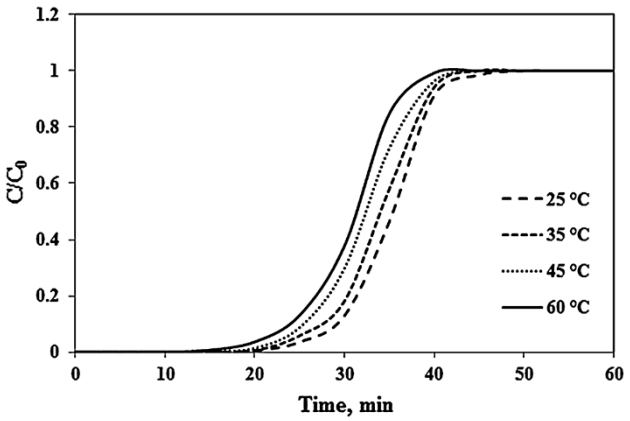

Fig. 3 CO_2 breakthrough curve for zeolite 4A at 1 bar

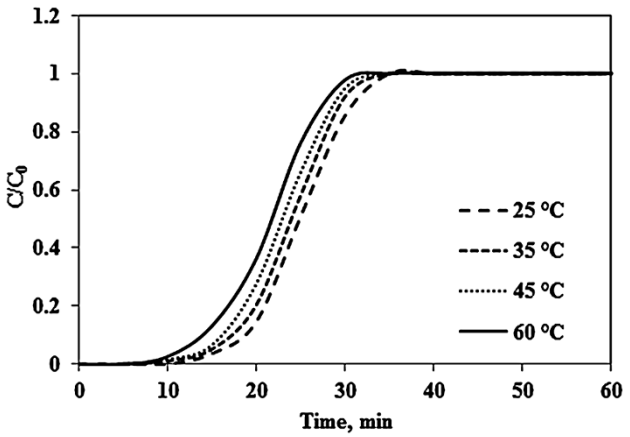

Fig. 4 CO_2 breakthrough curve for AC at 1 bar

Adsorption isotherms

In this study, the CO_2 adsorption for each adsorbent was measured under a series of isothermal conditions (i.e., 25, 35, 45 and 60 °C). It can be seen that all isotherm curves exhibit common behavior regardless of temperature and adsorbent type which mean the amount of CO_2 adsorbed on the adsorbent increases very rapidly with the increase in pressure over the low pressure range, and it tends to stabilize as the pressure continues to increase as shown in Figs. 5, 6 and 7. The isotherms behavior follows the type-I isotherm category according to IUPAC adsorption isotherm classification [26], which indicates a monolayer adsorption mechanism, commonly applied to micro-porous adsorbents.

The adsorption isotherms curves reveal the typical behavior showing the effect of temperature on the CO_2 adsorption capacity. That is, an increase in adsorption temperature leads to a reduction in the amount of adsorbed CO_2. Rising temperature simply provides more internal energy to CO_2 molecules in the gas phase. It should be noted that the increasing energy allows gaseous molecules to diffuse at a greater rate, but, at the same time, it reduces the chance for the CO_2 to be restrained or trapped by fixed energy adsorption sites on the adsorbent surface.

The amount of CO_2 adsorbed by using zeolite 13X is 4.215 $mol_{CO_2}kg^{-1}_{sorbent}$ while the amount of CO_2 adsorbed by using zeolite 4A is 3.263 $mol_{CO_2}kg^{-1}_{sorbent}$ at 1 bar and a temperature of 25 °C. AC gives the lowest adsorption capacity with an amount of 2.828 $mol_{CO_2}kg^{-1}_{sorbent}$ for this particular study. At higher temperature, CO_2 adsorption capacity for the adsorbents decreases by 20–30 %. In addition, the slope of adsorption isotherm curve reveals the strength of interaction between CO_2 molecules and the adsorption sites for individual sorbents. It appears that zeolite based adsorbents which exhibit greater slope of the adsorption curves have stronger adsorption sites as compare to AC. The experimental data were fitted to standard isotherm models like Langmuir and Freundlich model. The Langmuir isotherm equation can be represented as shown in Eq. 1 [27]

$$q = \frac{q_m K P_{CO_2}}{1 + K P_{CO_2}} \quad (1)$$

where q is the amount of CO_2 adsorbed at the CO_2 partial pressure P and q_m is the amount of CO_2 adsorbed with monolayer coverage. The values of q_m and Langmuir constant K, calculated from the CO_2 adsorption isotherms, are listed in Table 4. The monolayer CO_2 coverage at the different temperatures 25, 35, 45 and 60 °C were well-fitted for the zeolite adsorbents. While, Freundlich equation takes the form as shown in Eq. 2 [27]:

$$q = K P_{CO_2}^{1/n} \quad (2)$$

where K and n are Freundlich model constants. The K and n values of zeolite are higher than that of activated carbon. The Freunlich constant and regression co-efficient are given in Table 5 and agree well with AC.

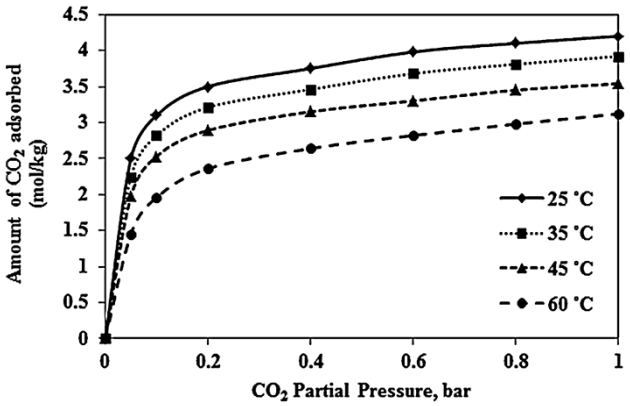

Fig. 5 CO_2 adsorption isotherms on zeolite 13X

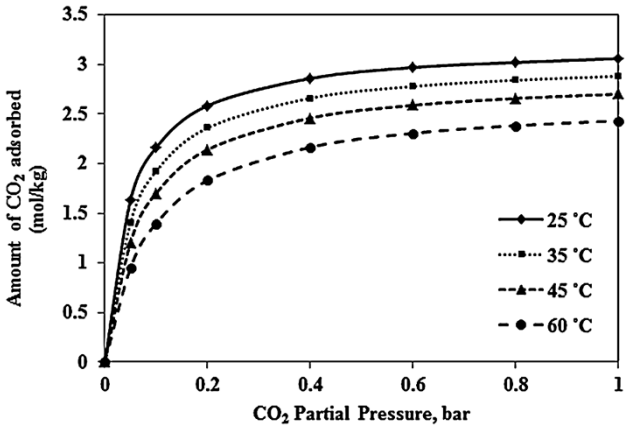

Fig. 6 CO_2 adsorption isotherms on zeolite 4A

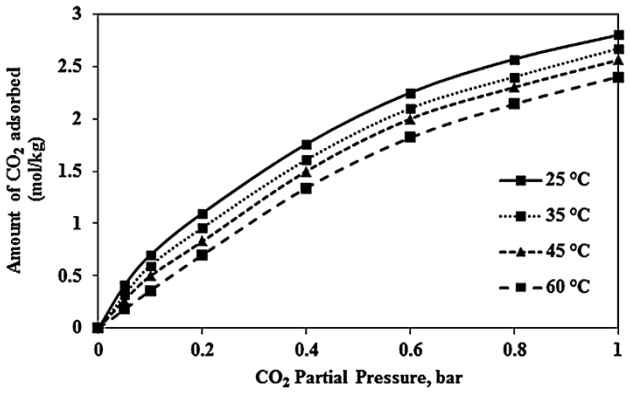

Fig. 7 CO_2 adsorption isotherm on AC

The average percent deviation quantity, Δq, or the adsorbed amounts were calculated using the following formula given in Eq. 3 [28]:

Table 4 Langmuir constants and their regression coefficient

Material	Temp (°C)	Langmuir constant		R^2	Δ q %
		q_m	K		
Zeolite 13X	25	4.245	19.031	0.987	6.6
	35	3.971	16.875	0.978	9.7
	45	3.521	13.747	0.987	8.5
	60	3.173	11.202	0.978	10.8
Zeolite 4A	25	3.263	19.031	0.997	5.4
	35	3.071	16.875	0.974	12.5
	45	2.921	13.747	0.979	7.9
	60	2.617	11.202	0.989	9.5
AC	25	2.828	21.956	0.961	9.8
	35	2.711	19.119	0.933	8.5
	45	2.591	15.502	0.948	12.7
	60	2.494	11.759	0.939	10.5

Table 5 Freunlich constants and their regression coefficients

Material	Temp (°C)	Freunlich constant		R^2	Δq %
		K	n		
Zeolite 13X	25	1.122	6.127	0.918	6.7
	35	1.034	5.483	0.938	10.5
	45	0.952	4.594	0.925	9.5
	60	0.836	3.812	0.973	12.3
Zeolite 4A	25	1.122	5.025	0.917	9.5
	35	1.034	4.386	0.923	11.2
	45	0.952	3.891	0.929	10.4
	60	0.836	3.311	0.937	9.7
AC	25	0.505	1.701	0.987	5.4
	35	0.447	1.551	0.982	8.4
	45	0.383	1.387	0.995	9.1
	60	0.346	1.319	0.986	6.7

$$\Delta q\% = \frac{100}{h}\sum_{j=1}^{h}\left|\frac{N^{\exp} - N^{\mathrm{cal}}}{N^{\exp}}\right| \quad (3)$$

where h is the number of experimental data and N^{exp} and N^{cal} are the experimental and calculated number of moles that are adsorbed by the adsorbent pellet.

Adsorption thermodynamics

The thermodynamic parameters are calculated from the Langmuir isotherms by using the Vant'Hoff's equation as follows in Eq. 4–6 [29]:

$$\Delta G^{\circ} = -RT\ln K_l \quad (4)$$

Table 6 Thermodynamic parameters for the adsorption of CO_2

Material	Temp (°C)	$\Delta G°$ (kJ/mol)	$\Delta H°$ (kJ/mol)	$\Delta S°$ (J/mol.K)
Zeolite 13X	25	−7.929	−11.274	17.568
	35	−7.689		
	45	−6.299		
	60	−6.236		
Zeolite 4A	25	−7.299	−12.852	18.499
	35	−7.236		
	45	−6.929		
	60	−6.689		
AC	25	−7.653	−14.98	24.379
	35	−7.556		
	45	−7.247		
	60	−6.824		

$$\Delta H^{\circ} = R\frac{T_1 T_2}{T_2 - T_1}\ln\frac{K_2}{K_1} \quad (5)$$

$$\Delta S^{\circ} = \frac{\Delta H^{\circ} - \Delta G^{\circ}}{T} \quad (6)$$

where ΔG° is change in the Gibb's free energy, ΔH° is change in the enthalpy and ΔS° is change in the entropy. A plot of ln K_{eq} vs. $1/T$ should be a straight line with a slope = $-\Delta H^{o}/R$ and an intercept = $\Delta S^{o}/R$ which is called Van't Hoff equation.

The thermodynamic parameters, Gibbs free energy change, $\Delta G°$ was calculated using Langmuir constants and the results are listed in Table 6. The enthalpy change, $\Delta H°$ and the entropy change, $\Delta S°$, for the CO_2 adsorption process on zoelite 13X are −11.274 kJ/mol and 17.568 J/mol·K respectively, while the enthalpy change and entropy change for zeolite 13X and zeolite 4A were calculated to give −12.852 kJ/mol and −18.499 J/mol·K respectively. For AC, enthalpy change, $\Delta H°$ and entropy change, $\Delta S°$ are −14.98 kJ/mol and −24.379 J/mol.K respectively. The negatives values of $\Delta G°$ confirm the feasibility of the process and the spontaneous nature of the adsorption process. The negative values in $\Delta H°$ indicated that the adsorption reaction is exothermic for all the adsorbents used. The positive value of $\Delta S°$ reflects the affinity of the adsorbents with CO_2 and suggests some structural change in CO_2 and the adsorbents.

Regeneration study

The three adsorbents were tested for material aging by using the same adsorbent over five adsorption desorption cycles at 25 °C and at 1 bar. The desorption process is achieved by increasing the bed temperature up to 100 °C which increases the internal energy of the gas and allowed the gas molecules to escape from the reactor. Figure 8 shows the adsorption isotherms of CO_2 zeolite 13X at 25 °C for five cycles. Up to 0.2 bar the CO_2 adsorption increased rapidly when the pressure was increased. The increase in CO_2 adsorption after 0.2 bar appeared to be gradual. The adsorption isotherms for repeated cycles showed a reduction in the amount of adsorption for the next cycles. This indicated that the adsorption is not reversible and complete regeneration cannot be obtained by adsorption of the material after adsorption. The amount of adsorption is almost similar for cycles 4 and 5 which indicate that the adsorbent is almost saturated with CO_2 (Table 6).

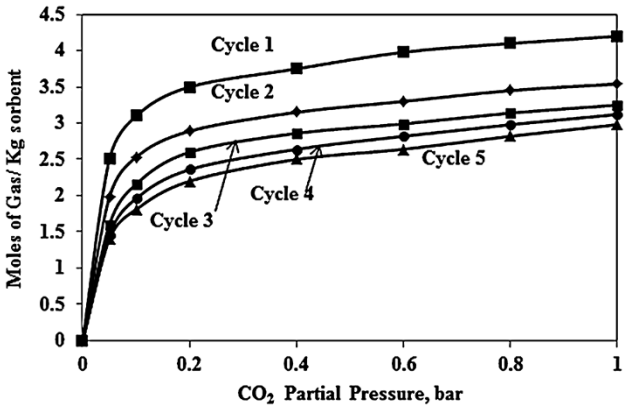

Fig. 8 Adsorption isotherms of zeolite 13X

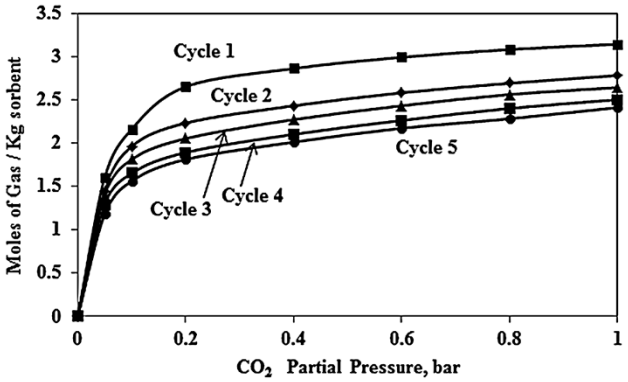

Fig. 9 Adsorption isotherms of zeolite 4A

The adsorption isotherms for zeolite 4A are shown in Fig. 9 and shows that the adsorption isotherms of CO_2 for zeolite 4A is not highly reproducible, indicating that the adsorption is not completely reversible. The adsorption at the first cycle was the highest. The uptake of CO_2 for molecular sieve 4A was lower than that of molecular sieve 13X at all pressures up to 1 bar. The adsorption isotherms for AC are shown in Fig. 10. It is interesting to note that all the isotherms are extremely reproducible, which indicates the excellent reversibility of adsorption. The CO_2 uptake for AC was lower than that of the two

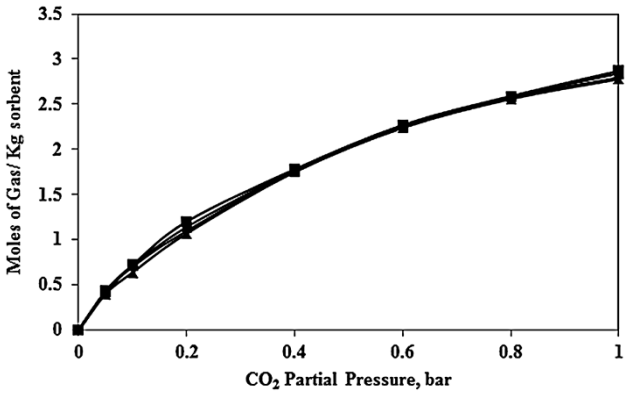

Fig. 10 Adsorption isotherms of AC

zeolite at lower pressures, but at higher pressures (up to 35 bar) the CO_2 uptake for AC was higher than that of the zeolites [25].

Conclusions

The CO_2 adsorption experiments were conducted using gravimetric method at different temperatures and pressures. From this study, it was concluded that the CO_2 adsorption isotherm obtained in this study followed general gas adsorption behavior, demonstrating that the CO_2 adsorption capacity increases with increasing pressure and decreases with increasing temperature. The adsorption isotherm follows a type-I isotherm classification according to IUPAC, representing a monolayer adsorption mechanism. Among the three adsorbents tested, zeolite 13X offers the highest adsorption capacity, and AC provides the lowest capacity at temperatures ranging from 25 to 60 °C and pressures up to 1 bar. The experimental data of CO_2 adsorption were fitted with Langmuir and Freunlich isotherm models. It was found that Langmuir model showed the best fit with the zeolite 13X and zeolite 4A while Freunlich model provided excellent fit with AC. The thermodynamics parameter were calculated from Van't Hoff's equation and concluded that the adsorption experiment were exothermic in nature for the three adsorbents. There is no full regeneration for zoelites while a full regeneration can be achieved with AC.

Authors' contributions All authors have been involved in drafting the manuscript and approved the final manuscript.

Acknowledgments This study has been funded by the Indian Institute of Technology Guwahati.

Conflict of interest The authors declare that there are no conflicts of interests regarding the publication of this article.

References

1. Song, C.: Global challenges and strategies for control, conversion and utilization of CO_2 for sustainable development involving energy, catalysis, adsorption and chemical processing. Catal Today **115**, 2–32 (2006)
2. Metz, B., Davidson, O., Coninck, H., de, Loos, M., Meyer, L.: Carbon dioxide capture and storage, International Panel on Climate Control. Cambridge University Press, IPCC) (2005)
3. Yang, H., Xu, Z., Fan, M., Gupta, R., Slimane, R.B., Bland, A.E., Wright, I.: Progress in carbon dioxide separation and capture: A review. J Environ Sci **20**, 14–27 (2008)
4. Self, et al.: Review of underground coal gasification technologies and carbon capture. Int J Energ Environ Eng **3**, 16 (2012)
5. Konduru, N., Linder, P., Assaf-Anid, N.M.: Curbing the greenhouse effect by carbon dioxide adsorption with zeolite 13X. Wiley Inter Sci **53**(12), 3137–3143 (2007)
6. Kuramochi, T., Faaij, A., Ramırez, A., Turkenburg, W.: Prospects for cost-effective post-combustion CO_2 capture from industrial CHPs. Int. J. Greenh. Gas. Control. **4**, 511–524 (2010)
7. Hurtado, A., Eguilior, S., Recreo, F.: Methodological development of a probabilistic model for CO_2 geological storage safety assessment. Int. J. Energy. Environ. Eng. **5**, 84 (2014)
8. Agarwal, A., Biegler, L.T., Zitney, S.E.: A super structure-based optimal synthesis of PSA cycles for post-combustion CO_2 capture. AIChE J **56**, 1813–1828 (2010)
9. Chue, K.T., Kim, J.N., Yoo, Y.J., Cho, S.H., Yang, R.T.: Comparison of activated carbon and zeolite 13X for CO_2 recovery from flue gas by pressure swing adsorption. Ind. Eng. Chem. Res. **34**, 591–598 (1995)
10. Sircar, S., Kratz, W.C.: Simultaneous production of hydrogen and carbon dioxide from steam reformer off-gas by pressure swing adsorption. Sep. Sci. Technol. **23**, 2397–2415 (1988)
11. Xu, X., Song, C., Miller, B.G., Scaroni, A.W.: Adsorption separation of carbon dioxide from flue gas of natural gas-fired boiler by a novel nanoporous "molecular basket" adsorbent. Fuel. Process. Technol. **86**, 1457–1472 (2005)
12. Drage, T.C., Arenillas, A., Smith, K.M., Pevida, C., Piippo, S., Snape, C.E.: Preparation of carbon dioxide adsorbents from the chemical activation of urea–formaldehyde and melamine–formaldehyde resins. Fuel **86**, 22–31 (2007)
13. Ribeiro, R.P.P.L., Grande, C.A., Rodrigues, A.E.: Activated carbon honeycomb monolith–Zeolite13X hybrid system to capture CO_2 from flue gases employing Electric Swing Adsorption. Chem. Eng. Sci. **104**, 304–318 (2013)
14. Cheung, O., Bacsik, Z., Liu, Q., Mace, A., Hedin, N.: Adsorption kinetics for CO_2 on highly selective zeolites NaKA and nano-NaKA. Appl. Energy **112**, 1326–1336 (2013)
15. Thang, H.V., Grajciar, L., Nachtigall, P., Bludsky, O., Areán, C.O., Frýdová, E., Bulánek, R.: Adsorption of CO_2 in FAU zeolites: Effect of zeolite composition. Catal. Today. **227**, 50–56 (2014)
16. Chen, C., Park, D.W., Ahn, W.S.: CO_2 capture using zeolite 13X prepared from bentonite. Appl. Surf. Sci. **292**, 63–67 (2014)
17. He, X., Lie, J.A., Sheridan, E., Hägg, M.B.: CO_2 Capture by Hollow Fibre Carbon Membranes: Experiments and Process Simulations. Energy Proced. **1**, 261–268 (2009)
18. Skarstrom: C. W. U.S. Patent 2, 944, 627 (1960)

19. Tlili, N., Grevillot, G., Vallieres, C.: Carbon dioxide capture and recovery by means of TSA and/or VSA. Int. J. Greenh. Gas Control **3**, 519–527 (2009)
20. Guerrin de M., Domine P.: D. U.S. Patent 3,155, 468 (1964)
21. Ruthven, D., Farooq, S., Knaebel, K.S.: Pressure swing adsorption, p. 352. VCH, New York (1994)
22. Adeyemo, A., Kumar, R., Linga, P., Ripmeester, J., Englezos, P.: Capture of carbon dioxide from flue or fuel gas mixtures by clathrate crystallization in a silica gel column. Int. J. Greenh. Gas Control **4**, 478–485 (2010)
23. Pugsley, T.S., Berruti, F., Chakma, A.: Computer simulation of a novel circulating fluidized bed pressure- temperature swing adsorber for recovering carbon dioxide from flue gasses. Chem. Eng. Sci. **49**(24A), 4465–4481 (1994)
24. Chue K., Jong-Nam K., Yun-Jong Y., Soon-Haeng C., in Fundamentals of Adsorption, ed. by LeVan, D., Kluwer Proc. Int. Conf., (Academic Publishers: Boston, MA, 1996) p. 203–210
25. Pellerano, M., Pre, P., Kacem, M., Delebarre, A.: CO_2 capture by adsorption on activated carbon by pressure modulation. Energy Procedia **1**, 647–653 (2009)
26. Keller, J.U., Staudt, R.: Gas adsorption equilibria: experimental methods and adsorptive isotherms. Springer Science and Business Media Inc, Boston (2005)
27. Guo, B., Chang, L., Xie, K.: Adsorption of carbon dioxide on activated carbon. J. Nat. Gas Chem. **15**, 223–229 (2006)
28. Morse, G., Jones, R., Thibault, J., Tezel, F.H.: Neural network modeling of adsorption isotherms. Adsorption **17**(2), 303–309 (2010)
29. Alzaydien, A.S., Manasreh, W.: Equilibrium, kinetics and thermodynamic studies on the adsorption of phenol onto activated phosphate rock. Int. J. Phy. Sci. **4**(4), 172–181 (2009)